Tribology and Materials
Vol. 1, No. 4, 2022, pp. 128-137

ISSN 2812-9717
https://doi.org/10.46793/tribomat.2022.016

Wear and flow rate problems on chutes in a rock crushing plant

Keshav GOPAUL *, Santaram VENKANNAH, Muhammad Zaid DAUHOO

University of Mauritius, Moka, Mauritius
*Corresponding author: keshav.gopaul1@gmail.com

Keywords
chutes
wear
hardness
discrete element method
abrasion
bulk material

History
Received: 10-12-2022
Revised: 27-12-2022
Accepted: 29-12-2022

Abstract

Rock crushing plants cannot afford unforeseen breakdowns with the current boom in the construction sector. This paper discusses measures that can be used to predict wear on chutes in the plant so that predictive maintenance can be implemented. Some of the chutes used to transfer the materials are difficult to access. Failures of the chutes cause downtimes, which are untimely and costly. The objective of this research is to determine the wear rates of chutes. A chute system was designed, modelled and validated using the Solidworks® software and then imported into the EDEM® software to predict the failure of the chutes. Factors affecting the abrasion wear of the metal were determined and used as input parameters to perform a simulation on EDEM® to validate the wear recorded. The service life obtained for mild steel S275 was 731 hours and that of abrasion resistant steel Hardox® 400 was 1490 hours, and it was deduced that the difference in the value of hardness of the metals to that of the rocks they carry significantly affects the wear of the chutes. The software was also used to replicate the flow of boulders on chutes and an accelerated flow rate of 496 tons per hour (t/h) was achieved at an angle of elevation of 24.4°.

1. Introduction

Transportation of materials during the rock crushing process is performed by conveyors and chutes. The major issue with chutes is the occurrence of wear often leading to major breakdowns [1]. Moreover, the flow rate of material through chutes is not always optimal. Common chute geometries are "U-shaped" or "ducted" types [2]. Depending on the nature of the bulk material being transferred, the chute material is selected. However, the most common type of chute material is mild steel or stainless steel. In chute manufacturing, the thickness of the plate is chosen based on the type of bulk material, the amount of material required to flow, structural stability and also the allowable limit of wear (when no lining materials are to be used).

Two categories of flows occur on chutes namely: slow flow and fast flow. Slow flow of bulk material takes place when the material is transferred with a constant depth (H) and at a constant velocity, as shown in Figure 1a. Fast flow occurs when the material accelerates down the chute. In this case, the height of the bed decreases along the length of the chute as illustrated in Figure 1b [3].

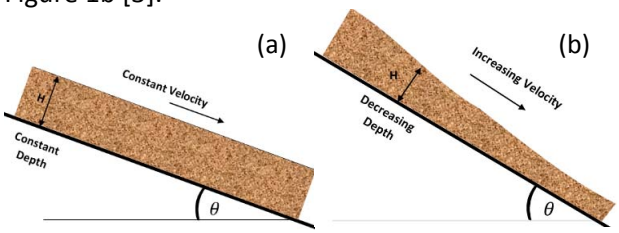

Figure 1. Categories of flows occur on chutes: (a) slow flow and (b) fast flow

In the case of fast flow, if the length of the chute is long enough, the material may flow with terminal velocity when steady state flow can be achieved [4]. With sufficient exposure time, with the flow of bulk material, two types of wear occur on chutes, namely: impact abrasion wear and abrasion wear (sliding wear) [5,6]. At locations where the material is discharged onto the chutes, the surface is exposed to impact abrasion wear, which occurs

when the relative motion of the flowing particle is almost normal to the surface, as shown in Figure 2a. Sliding abrasion wear occurs when the relative motion of the flowing particles is almost parallel to the chutes' surface, as shown in Figure 2b [7].

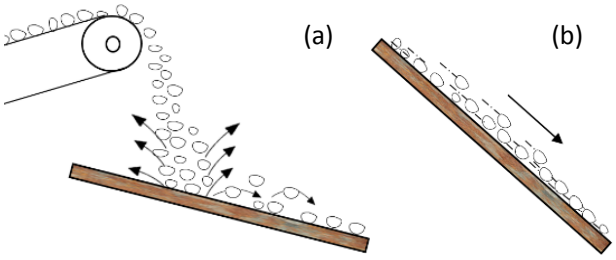

Figure 2. Types of wear occur on chutes: (a) impact wear and (b) sliding wear

The rate at which chute surfaces are abraded is heavily dependent on several factors [8]. Understanding the effect of these factors is primordial for developing a strategy to predict the wear rate as well as the service life of chute materials. The development of strategies capable of predicting the wear rate and the service life of chute material will reduce unpredictable breakdowns of plants. Moreover, the cost associated with unscheduled maintenance will be saved and an appropriate selection of lining material can be done which will ensure the longevity of the system.

The abrasive wear of material subjected to the flow of the different types of bulk material under both "slow" and "fast" flow conditions on chutes can be determined using Equation (1) [9].

$$W_L = \frac{M \cdot 10^3}{A\rho}, \quad (1)$$

where W_L is the linear wear (μm), M is the mass loss (g), A is the contact surface area (m^2) and ρ is the density (kg/m^3).

However, with the emancipation of technology, the discrete element method (DEM) has become a reliable and powerful tool to study and predict the flow of particles. This methodology is being widely used in research related to bulk handling processes. It has become possible to optimise the design of equipment, such as conveyors, chutes and vibrating screens by DEM [10]. The advantages of this method are that it provides accurate and time-saving results. Moreover, no human intervention is required which makes it a safer process. A software, which is extensively used is EDEM®, which is designed to build a computational model to resolve issues in bulk handling processes. A set of DEM parameter values are determined and input to the software to replicate actual conditions which can thereafter be used to predict wear in bulk solids handling [11,12]. DEM parameters are usually classified into four categories namely: particle, geometry, contact and simulation parameter. Some values are determined through laboratory experiments [13], while others are through research [14-17].

This paper presents a study on the predictability of wear of chutes at a rock crushing plant in Mauritius. Timely maintenance of chutes will reduce major breakdowns, which leads to unscheduled maintenance, especially on difficult-to-access parts of the conveyors. The study also considers the redesign of chutes to optimise the flow rate of boulders. At the factory, chutes are manufactured locally and the material commonly used for manufacturing the chutes is mild steel due to its relatively cheap price, availability and good machinability and weldability. The company protects its chute with Hardox® 400 (HX 400), which are abrasion resistant steel plates with a partial chemical composition shown in Table 1. These plates are used to reduce the wear rate and are bolted to the mild steel S275 (EN 10025) chutes surface. Some basic mechanical properties of these two types of metal plates are compared in Table 2.

Table 1. Chemical composition of HX 400 [18]

Element	C	Si	Mn	Cr	Ni	Mo
wt. %	0.32	0.70	1.60	2.50	1.50	0.60

Table 2. Mechanical properties of S275 and HX 400 [18,19]

Property	S275	HX 400
Yield strength, MPa	275	1000
Tensile strength, MPa	410	1250

Moreover, the hardness of HX 400 plates is approximately 2.5 times more than that of S275 (mild steel). Even with HX 400 plates attached to the chutes, it has been observed that the wear rates of these plates are relatively high which often leads to frequent breakdowns. Furthermore, the flow rate of bulk material on one specific chute towards crushing equipment is observed to be unsatisfactory. This makes the performance of the crushing equipment less efficient as it has been designed to sustain a much higher flow rate of material, which was not achieved in practice within normal operating hours. There cost associated with unexpected breakdowns causing unscheduled intervention or maintenance due to wear on chutes and lower production is significant prompting the

company to seek practical solutions. Hence, it has become important to perform an investigation on this matter to reduce these non-value-added costs.

The trial and error approach is not an effective solution and the research team proposed a simulation of the system to determine a feasible solution that can be used to shorten the redesign time. The model requires validation first and data on the current system have to be collected and analysed. Laboratory experiments were performed to determine the values of the main factors affecting the abrasion wear of the metal. The chute system was then modelled on Solidworks® software and then imported on the EDEM® for simulations.

2. Methodology

2.1 Wear rate of material by experimentation

To achieve the aim of the study related to the occurrence of wear on chutes, the chute material, mild steel and its lining material HX 400 were utilised to perform an investigation. Their wear behaviour on chutes was studied to predict their service life, which would be useful information to reduce breakdowns. Hence, one specific chute where the highest wear was observed was selected. That chute is referred to as HP 300 No. 1. The chute usually transports basalt rocks of size ranging between 31 to 50 mm in diameter.

The number of metal samples was chosen so both types of wear could be investigated. To study the effect of both, sliding and impact wear of metals on chutes the samples were placed at two different positions on the chute and subjected to the same flow rate over the same period. A mild steel sample was next to an HX 400 one at each position covering the whole width of the chute to ensure continuous flow without any obstacles. Thus, a total of 4 samples: two made of mild steel and two of HX 400 were needed. The mass of each sample was recorded before welding them in the configuration shown in Figure 3.

The metal samples were then exposed to the flow of the bulk material for 32 days, after which the samples were retrieved. The weld slags were then removed by gently hammering with a chipping hammer to avoid altering the mass of the samples. Their final masses were measured using a balance, with a precision of 0.001 kg. The wear was measured in terms of the mass loss and converted into average linear wear of the samples using Equation (1) with the value of density of metals obtained from the manufacturer's specification.

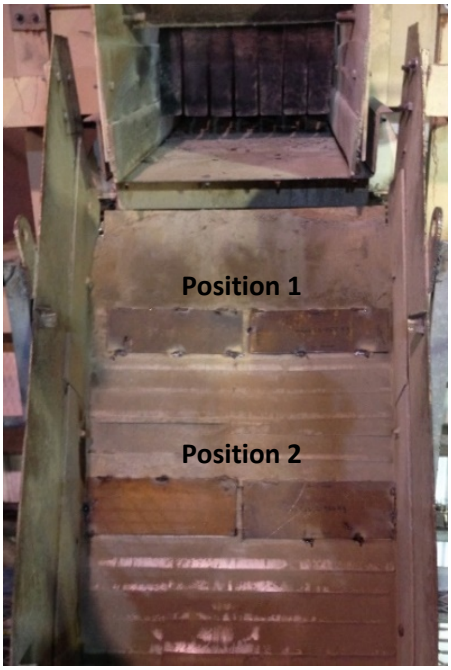

Figure 3. Arrangement of samples on chutes

2.2 Mass flow rate

The mass flow rate was determined by reviewing data collected from the crushing plant. The plant usually operates from 07:00 to 19:00. However, some assumptions were made to calculate an average mass flow rate per day which are as follows: the values set by the operator were similar for each day; the value to which the mass flow rate was set was the same at which the bulk material flows with on the chute.

A systematic sampling technique was used by reviewing the flow rate set each hour. The values reviewed from the data logger are given in Table 3. The calculated average mass flow rate was 403.33 t/h, i.e. 112.04 kg/s.

Table 3. Mass flow rates collected from the factory

Time of operating	Mass flow rate, t/h
07:00	350
08:00	380
09:00	380
10:00	420
11:00	420
12:00	420
13:00	450
14:00	450
15:00	450
16:00	400
17:00	400
18:00	320

2.3 Hardness of material and particles

Chutes' material and particle hardness were determined using a portable hardness tester [20]. First, the surfaces of each test piece were polished using the grinding polishing method to remove any oxide layer present and hence, ensure a flat surface. Figure 4 shows the hardness test pieces ready to be tested.

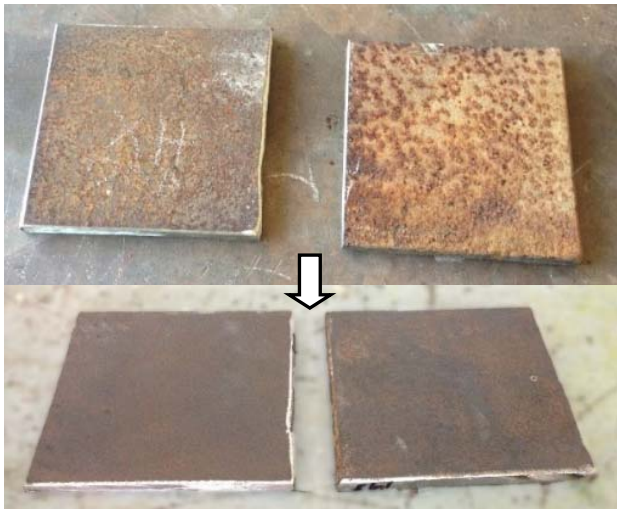

Figure 4. Hardness test samples

Before performing the tests, the apparatus was calibrated using the standard test block provided by the manufacturer. This ensured that the apparatus is fully functional. The hardness of the samples and basalt rock were then measured. Rock samples were readily available at the factory's laboratory.

2.4 Abrasion resistance

The abrasion resistance was determined by the Los Angeles abrasion test as shown in Figures 5 and 6, in accordance with the ASTM C131 standard [21]. The sample to carry out the test was prepared as follows. A sieve with an aperture size of 31.5 mm was used to eliminate undersized particles and a 50 mm size to remove oversized particles. Hence, particle sizes in the range of 31.5 mm to 50 mm were obtained as a sample. The sample was washed and oven-dried at 105 °C to substantially constant mass. The mass of the sample was measured using a sensitive electronic balance and recorded to the nearest 1 g (m_1), as shown in Figure 5.

The sample and steel spheres were placed in the Los Angeles testing machine as illustrated in Figure 6 and the machine was rotated at a speed of 33 rpm for 1000 revolutions. After 1000 revolutions, the material was discharged from the machine and a preliminary separation of the

Figure 5. Initial weighting of the test sample

sample was done using a sieve coarser than 1.70 mm. The finer portion of the material was sieved on a 1.70 mm sieve. Material coarser than 1.70 mm was washed. The material was oven-dried again at 105 °C to substantially constant mass and weighed to the nearest 1 g again (m_3), so the percent loss (LA value) is calculated as:

$$\text{LA value} = \left(\frac{m_1 - m_3}{m_1} \right) \cdot 100\ \%. \qquad (2)$$

Figure 6. Test sample along with steel spheres

2.5 Wear rate of chute materials by simulation

DEM parameters determined either from literature or through experimentation or obtained directly from the factory's laboratory were used as input parameters on the EDEM® to create and replicate a realistic flow of material on chutes.

A virtual chute with metal samples attached to it and rock particles compactly filled with solid spheres were created as shown in Figure 7. Some of the physical properties used in the simulation were determined through experimentation and others were obtained from references as discussed in section 3.2.

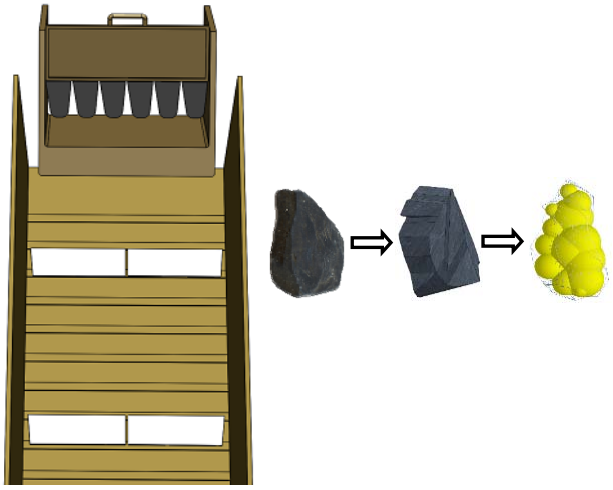

Figure 7. Virtual model of the chute and rock particle

The flow rate issue was related to the flow of bigger-sized particles known as boulders. Virtual models of these boulders and the chute transporting them were created as illustrated in Figure 8. The same set of DEM parameters representing the actual properties of bodies concerned was input to EDEM® to replicate the flow of boulders at factory conditions. Recent research conducted [22], revealed that the governing parameter of the flow rate of material on chutes is the angle of inclination, also known as the "chute angle". Hence, small increments of 0.2° were made to the present value of the chute angle to obtain a set of optimum parameters to which the chute needs to be redesigned. It should be noted that an allowable value of wear rate was set as a limit to which the chute angle can be increased.

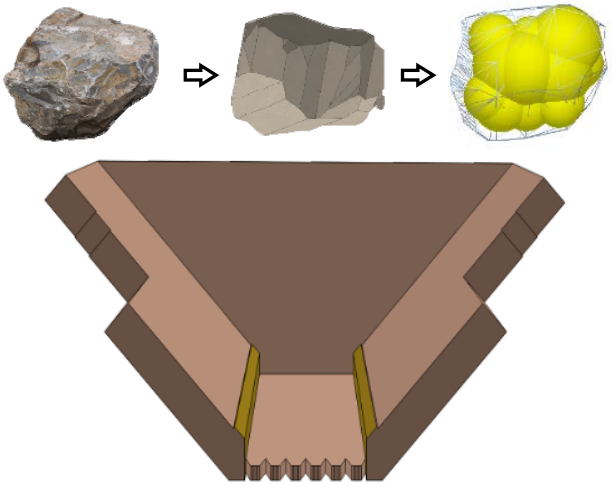

Figure 8. Boulder and chute model

3. Results and analysis

The results are based on 32 days of exposure of the metal samples to the flow of material on the chute with a total of 221.36 hours of operation.

3.1 Linear wear of mild steel and HX 400 plates

Figures 9 and 10 show the samples initially exposed which are compared to the samples retrieved after 32 days of exposure at the chute.

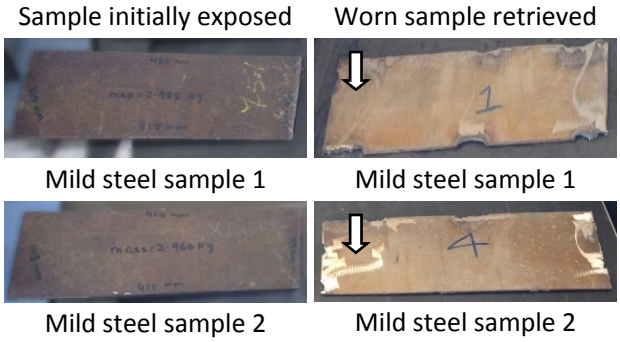

Figure 9. Mild steel samples visual comparison (arrow indicates the direction of the bulk material flow on the sample)

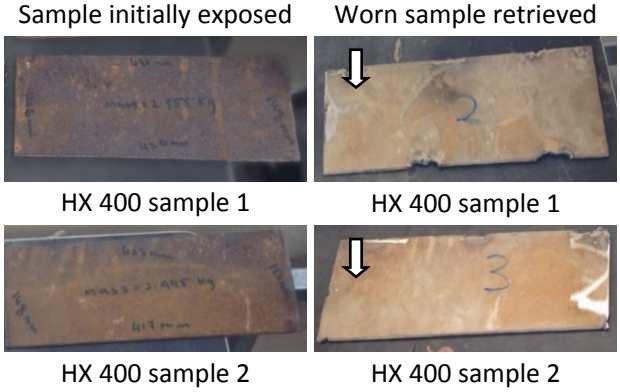

Figure 10. HX 400 samples visual comparison (arrow indicates the direction of the bulk material flow on the sample)

The initial reading on the hour meter at the factory was recorded before starting the experiment and the same reading was recorded after 32 days of exposure to the flow of bulk particles. It was deduced that the chute was in operation for T = 221.36 hours, i.e. 796,896 seconds.

An example of how the wear rate and service life for mild steel sample 1 was calculated is provided below. The linear wear obtained for the sample was 1962 µm. Therefore, the wear rate can be determined as follows:

$$\text{Wear rate} = \frac{W_L}{T} = \frac{1962}{221.36} = 8.86 \text{ µm/h}. \quad (3)$$

The initial thickness of the sample previously measured was 6480 mm. The service life can be calculated as follows:

$$\text{Service life} = \frac{6480}{8.86} \approx 731 \text{ h}. \quad (4)$$

The initial thicknesses of all the samples were similar but not exactly equal. Similar calculations of the wear rates and the service lives after the exposure of the samples on the chute were performed for the other samples and compared in Table 4. It can be observed from the results that mild steel sample 1 was severely worn out compared to the HX 400 sample 1 which was placed next to it. It was deduced that at position 1, the service life of mild steel is more than 3 times shorter than that of HX 400. This same trend was witnessed at position 2. It was also noticed that for the plate of the same material, the one placed at position 1 was worn approximately two times faster than the one at position 2. For instance, mild steel at position 1 has a service life of 731 hours and at position 2 it was 1490. The main reason for this difference is that the samples at position 1 were subjected to both, impact abrasion and sliding abrasion wear when rocks were discharged directly onto them, whereas those at position 2 were subjected only to sliding abrasion wear. Moreover, at both positions, the wear rate of mild steel was higher than that of HX 400. This confirms the change in thickness observed from the visual inspection.

Table 4. Service lives of metals samples at the chute

Sample type	Linear wear, µm	Wear rate, µm/h	Service life, h
Mild steel sample 1	1962	8.86	731
HX 400 sample 1	570	2.57	2400
Mild steel sample 2	888	4.01	1490
HX 400 sample 2	316	1.43	4329

A set of 20 values of the hardness of basalt rock and metals used as samples was recorded. The minimum, maximum and average values recorded by the portable hardness tester are shown in Table 5. Past studies have demonstrated that severe wear occurs when the hardness of the surface is 0.8 times less than the hardness of the abrasive and mild wear usually occurs when the hardness of the surface is between 0.8 and 1 times the hardness of the abrasive [23].

Table 5. Hardness of basalt rock and metals used

Type of surface	Minimum hardness HBW	Maximum hardness HBW	Average hardness HBW
Basalt rock	502	604	552
HX 400	378	424	406
Mild steel	105	232	144

From Table 5, it can be noticed that the average hardness of the basalt is 552 HBW. Hence, to observe mild wear, the hardness of the metal surface should lie between 441.6 and 552 HBW. However, for mild steel the average hardness recorded was 144 HBW, which is significantly lower compared to the minimum value of 441.6 HBW, required for mild wear [24]. This huge difference in hardness, explains why the mild steel sample experienced severe wear at both positions. For HX 400 the average hardness recorded was 406 HBW. This explains why relatively lighter wear was observed as compared to the mild steel samples.

The value of the mass flow rate obtained was 112.04 kg/s as per data collected in Table 3. Moreover, the abrasion resistance of the particles was found and is given in Table 6.

Table 6. Los Angeles abrasion test results

Initial mass, g	Mass before washing, g	Mass after drying, g	LA value, %
10,000	8981	8967	10.33

3.2 Modelling the wear issue

The experimental results of factors such as the mass flow rate and LA abrasion test were used as direct input to EDEM® whereas the hardness measurement of the surface was used to compute the wear coefficient and then input to the software to obtain the linear wear of the virtual samples. Table 7 summarises the inputs to EDEM®.

Figure 11 shows the use of a mass flow rate sensor to monitor and validate the flow along with the visual result of wear on each sample, with the red colour visually representing the regions on the samples with high wear.

Since the simulation provided satisfactory results, the wear data were exported from EDEM®. A linear relationship was developed between the linear wear and the service life for each sample, with the gradient representing the wear rate. An example related to mild steel sample 1 is provided in Figure 12.

From Figure 12, the equation of the regression line obtained was $Y = 2.1588 \times 10^{-6}\ X - 3.8399 \times 10^{-7}$ for mild steel sample 1, where Y is the linear wear and X is the time. The gradient of the best fit line represents the wear rate of the sample in mm per second. For comparison purposes with the experimental results, a unit conversion was done for the gradient, i.e. 2.1588×10^{-6} mm/s ≈ 7.77 µm/h.

Table 7. Input for simulation*

DEM parameter	Value	Source
Particle properties for basalt rock		
Poisson's ratio	0.3	factory
Density, kg/m^3	1300	
Modulus of elasticity, GPa	79.9	
Mass of rocks, kg	0 – 0.4	
Mass of boulders, kg	0 – 1500	
Size distribution	random	
Minimum radius, mm	15.75	
Minimum radius for boulders, mm	300	
Maximum radius, mm	25	
Maximum radius for boulders, mm	500	
Resistance to fragmentation, %	10.33	experiment
Geometry properties for chute		
Density, kg/m^3	7850	[25]
Modulus of elasticity, GPa	210	
Poisson's ratio	0.303	
Work function, eV	4.47	[14]
Hardness of mild steel HBW	144	experiment
Hardness of HX 400 HBW	406	
Interactions between particle to particle		
Coefficient of restitution (normal)	0.500	[15]
Coefficient of restitution (tangential)	0.200	[17]
Coefficient of static friction	0.100	[16]
Interactions between particle to geometry		
Coefficient of restitution (normal)	0.500	[12]
Coefficient of restitution (tangential)	0.010	
Coefficient of static friction	0.010	
Wear constant of mild steel × 10^{-13}, Pa^{-1}	3.926	calculated [26]
Wear constant of HX400 × 10^{-13}, Pa^{-1}	1.799	
Particle factory		
Factory type	unlimited	–
Target mass, kg/s	112.04	factory

Table 7. *Continued*

DEM parameter	Value	Source
Physics for particle to particle		
Contact model	Hertz-Mindlin (no slip)	EDEM®
Physics for particle to geometry		
Contact model	Hertz-Mindlin with linear wear	EDEM®
Simulation		
Time step Δt, s	30 % of RTS	EDEM®
Cell size	2.5 R_{min} (10 mm)	
Total simulation time, s	30	based on flow animation

*resistance to fragmentation – Los Angeles abrasion test results; particle factory – parameters connected with the generation of the particles; target mass – average mass flow rate; RTS – Rayleigh time step; R_{min} – minimum particle radius in the simulation.

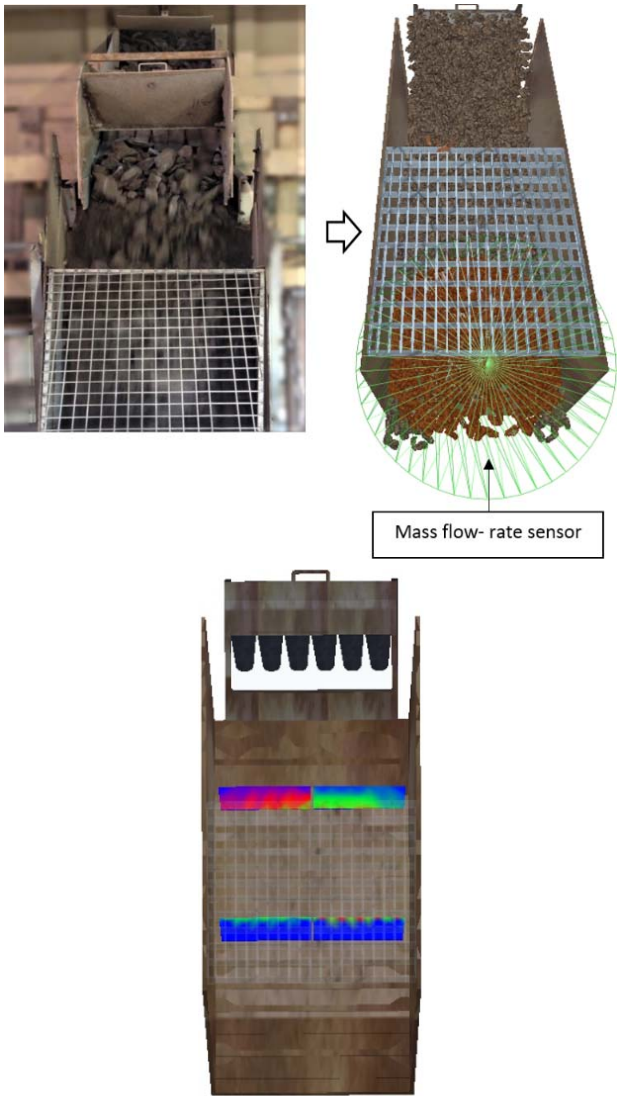

Figure 11. Wear map on samples after 30 s

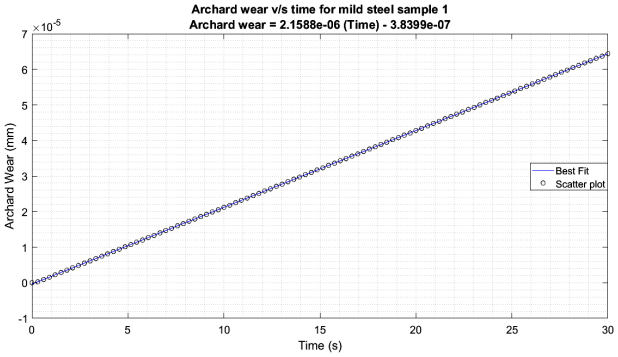

Figure 12. Linear (Archard) wear vs. time graph

The service life of mild steel sample 1 having an initial thickness of 6480 µm by simulation is therefore:

$$\text{Service life} = \frac{6480}{7.77} \approx 834 \text{ h.} \quad (5)$$

Hence, the service lives of chute material and its lining material could be predicted by knowing their initial thickness. Similar steps were repeated for the other samples and the results are presented in Table 8.

Table 8. Wear rate and service life by simulation

Sample type	Wear rate, µm/h	Service life, h
Mild steel sample 1	7.77	834
HX 400 sample 1	3.67	2821
Mild steel sample 2	2.19	1629
HX 400 sample 2	1.29	4789

Table 8 provides the results of the analysis performed on the virtual samples with the average hardness values of both the particle and metal surfaces. It can be noticed that the service lives obtained have the same trend as the experimental results. For instance, mild steel samples at both positions experienced more severe wear as compared to HX 400 ones. In addition, for the same metal at two different positions, the service life of the one at position 2 is twice longer than at position 1.

However, with the average hardness values the service life obtained by simulation exceeds the experimental ones. Therefore, to acquire more consistent results with the experimental values, additional simulations were performed with different scenarios related to the hardness values (as provided in Table 5) of both the particle and the metal surfaces. The most consistent results (Table 9) to the experimental ones were obtained when the hardness values for the metal samples were kept constant at the average value and the maximum hardness obtained for basalt rock was selected.

Table 9. Additional simulation results

Sample type	Service life scenario	
	experimental	with maximum hardness of basalt rock
Mild steel sample 1	731	764
HX 400 sample 1	1490	1491
Mild steel sample 2	2400	2583
HX 400 sample 2	4329	4385

The slight difference between the actual and modelled wear rate is explained since some factors such as a rise in temperature or contact angle of particles with the surface that affects the wear of the chute were not considered in the simulation.

3.3 Flow rate of boulders

The purpose of accelerating the flow of boulders towards crushing equipment was to increase its production rate. Simulations were first performed with the actual chute angle to obtain the current flow rate as shown in Figure 13 and to validate the other DEM parameters as well.

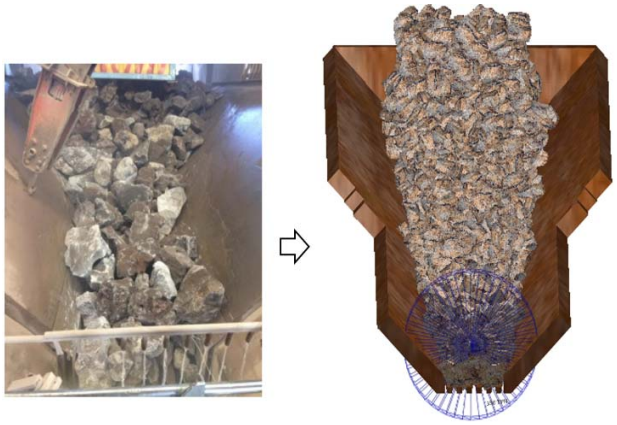

Figure 13. Boulders flow

Once the current flow rate was successfully obtained, the chute angle was increased in increments of 0.2° from the initial value, as shown in Figure 14, and simulations were performed. The objective was to achieve a set of optimum conditions to redesign the chute. It should be noted that a limit was set for acceptable wear of 8.86 µm/h based on the results obtained since increasing the mass flow rate increases the wear rate. Thus, the angle was increased until the wear rate was reached and the corresponding mass flow rate was displayed on the mass-flow rate sensor.

The set of conditions achieved is compared to the initial one in Table 10.

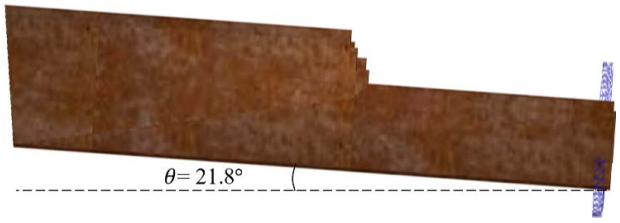

Figure 14. Initial inclination of the chute

Table 10. Additional simulation results and increase in mass flow rate of boulders

Chute angle, °	Wear rate, µm/h	Mass flow rate, t/h
21.8	2.71	350
24.4	8.86	496

Referring to Table 10, at the maximum allowable wear rate, the set of optimum conditions pertained to an angle of elevation of 24.4° since at that rate, the limit, 8.86 µm that was set for maximum wear rate is not exceeded. Thus, redesigning the chute with an angle of 24.4° would increase the flow rate of the boulders from 350 to 496 t/h, making the crushing equipment much more efficient.

3.4 Wear simulation

Figure 15 illustrates the wear map on the surface of the chute with a chute angle of 24.4°. It can be deduced that the regions of severe wear are at the point where the boulders are discharged onto the chute with repeated percussion on the surface. Hence, it would be beneficial to reinforce the surface at that location to prevent severe wear that leads to breakdowns, if the mass flow rate of 496 t/h was to be achieved.

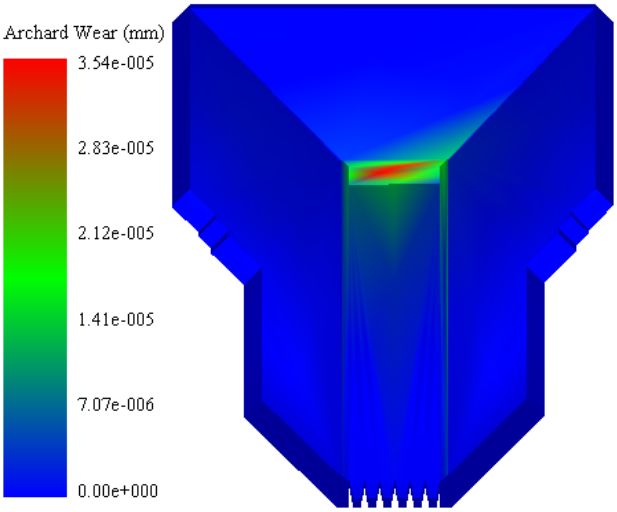

Figure 15. Wear map at optimum conditions after 10 seconds

4. Conclusion

It was observed that the difference between the hardness of the chute material and that of the abradant has been the main cause of the wear of the chutes. Essential information about the service life of the same metal at different positions on the chute was obtained. The importance of protecting chutes has also been demonstrated. Performed simulations have made possible the prediction of the service life of chute material with its initial thickness known. Furthermore, to prolong the service of chutes studied, harder materials than Hardox® 400 can be used, such as Abracorr® 600. Abracorr® 600 has a hardness greater than that of the particle and hence, it would be effective to be used for wear plates.

The flow of rocks on chutes was recreated on EDEM® and an optimum set of design parameters was obtained to redesign the chute carrying boulders. A chute angle of 24.4° is expected to increase the mass flow rate of boulders from 350 to 496 t/h. However, it was noticed that the discharge spot needs to be reinforced when redesigning. With the use of a material of higher hardness, the wear resistance of the lining material is expected to improve and lead to a decrease in unscheduled maintenance and cost. Also, redesigning chutes with optimum value of parameters is expected to increase the efficiency of crushing equipment and eventually that of the whole crushing plant as the flow rate would increase by 146 t/h. Therefore, allowing the crushing plant to meet its daily production target within normal operating hours. The existing system has been simulated and validated experimentally. The proposed changes including the new chute angle show that the uptime of the system can be increased while the flow rate can be increased before the failure of the chutes.

The model can be used to predict the wear rate and the flow rate in a system if the hardness of the chute material is known. This will allow the scheduling of stoppages of the line for the maintenance of components with minimum disruptions to the manufacturing systems.

Acknowledgement

Our thanks go to the University of Mauritius and to the directors of the rock crushing plant for allowing us to carry out this study on the crushing units, to access laboratories and for providing us with all facilities for the proper ongoing of this project. Our sincere gratitude to the technical team for helping us prepare the metal samples.

References

[1] R. Xia, X. Wang, B. Li, X. Wei, Z. Yang, Discrete element method- (DEM-) based study on the wear mechanism and wear regularity in scraper conveyor chutes, Mathematical Problems in Engineering, Vol. 2019, 2019, Paper 4191570, DOI: 10.1155/2019/4191570

[2] T. Barker, C. Zhu, J. Sun, Exact solutions for steady granular flow in vertical chutes and pipes, Journal of Fluid Mechanics, Vol. 930, 2022, Paper A21, DOI: 10.1017/jfm.2021.909

[3] C.R. Woodcock, J.S. Mason, Bulk Solids Handling, Blackie Academic & Professional, London, 1987, DOI: 10.1007/978-94-009-2635-6

[4] J. Rozentals, Flow of bulk solids in chute design, available at: http://www.ckit.co.za/secure/conveyor/papers/bionic-research-1/c-bri1-paper02.htm, accessed: 13.11.2022.

[5] M.J. Neale (Ed.), The Tribology Handbook, Butterworth-Heinemann, Oxford, 1995.

[6] A.R. Chintha, Metallurgical aspects of steels designed to resist abrasion, and impact-abrasion wear, Materials Science and Technology, Vol. 35, No. 10, 2019, pp. 1133-1148, DOI: 10.1080/02670836.2019.1615669

[7] A. Vencl, I. Bobić, B. Bobić, K. Jakimovska, P. Svoboda, M. Kandeva, Erosive wear properties of ZA-27 alloy-based nanocomposites: Influence of type, amount, and size of nanoparticle reinforcements, Friction, Vol. 7, No. 4, 2019, pp. 340-350, DOI: 10.1007/s40544-018-0222-x

[8] A. Monga, S. Gumber, H. Grover, Study of abrasion wear and factors affecting wear rate, International Journal of Advance Research in Science and Engineering, Vol. 7, No. Special Issue 6.04, 2018, pp. 113-120.

[9] A.W. Roberts, S.J. Wiche, Prediction of lining wear life of bins and chutes in bulk solids handling operations, Tribology International, Vol. 26, No. 5, 1993, pp. 345-351, DOI: 10.1016/0301-679X(93)90071-8

[10] F. Kessler, M. Prenner, DEM – Simulation of conveyor transfer chutes, FME Transactions, Vol. 37, No. 4, 2009, pp. 185-192.

[11] G. Chen, G. Lodewijks, D.L. Schott, Numerical prediction on abrasive wear reduction of bulk solids handling equipment using bionic design, Particulate Science and Technology, Vol. 37, No. 8, 2019, pp. 964-973, DOI: 10.1080/02726351.2018.1480547

[12] M.C. Marinack Jr., R.E. Musgrave, C.F. Higgs III, Experimental investigations on the coefficient of restitution of single particles, Tribology Transactions, Vol. 56, No. 4, 2013, pp. 572-580, DOI: 10.1080/10402004.2012.748233

[13] W. Chen, S. Biswas, A. Roberts, J. O'Shea, K. Williams, Abrasion wear resistance of wall lining materials in bins and chutes during iron ore mining, International Journal of Mineral Processing, Vol. 167, 2017, pp. 42-48, DOI: 10.1016/j.minpro.2017.08.002

[14] Work functions for photoelectric effect, available at: http://hyperphysics.phy-astr.gsu.edu/hbase/Tables/photoelec.html, accessed: 02.02.2022.

[15] Rocscience coefficient of restitution table in RocFall, available at: https://www.rocscience.com/help/rocfall/documentation/slope/materials/reference-tables/rocscience-coefficient-of-restitution-table-in-rocfall, accessed: 02.02.2022.

[16] E.H. Rutter, C.T. Glover, The deformation of porous sandstones; are Byerlee friction and the critical state line equivalent?, Journal of Structural Geology, Vol. 44, 2012, pp. 129-140, DOI: 10.1016/j.jsg.2012.08.014

[17] R.A. Schultz, Brittle strength of basaltic rock masses with applications to Venus, Journal of Geophysical Research: Planets, Vol. 98, No. E6, 1993, pp. 10883-10895, DOI: 10.1029/93JE00691

[18] Hardox® 400 data sheet, available at: https://www.ssab.com, accessed: 02.02.2022.

[19] BS EN 10025-2, Hot Rolled Products of Structural Steels – Part 2: Technical Delivery Conditions for Non-alloy Structural Steels, 2019.

[20] S. Gutt, G. Gutt, T.-L. Severin, M. Poroch-Seritan, S. Mironeasa, M.A. Oroianu, Portable hardness tester, in Proceedings of the 22nd International DAAAM Symposium, 23-26.11.2011, Vienna, Austria, pp. 699-700.

[21] ASTM C131/C131M-20, Standard Test Method for Resistance to Degradation of Small-Size Coarse Aggregate by Abrasion and Impact in the Los Angeles Machine, 2020.

[22] A.J. Holyoake, J.N. McElwaine, High-speed granular chute flows, Journal of Fluid Mechanics, Vol. 710, 2012, pp. 35-71, DOI: 10.1017/jfm.2012.331

[23] M.A. Moore, A review of two-body abrasive wear, Wear, Vol. 27, No. 1, 1974, pp. 1-17, DOI: 10.1016/0043-1648(74)90080-5

[24] G. Pintaude, F.G. Bernardes, M.M. Santos, A. Sinatora, E. Albertin, Mild and severe wear of steels and cast irons in sliding abrasion, Wear, Vol. 267, No. 1-4, 2009, pp. 19-25, DOI: 10.1016/j.wear.2008.12.099

[25] S.K. Jha, Investigation of micro-structure and mechanical properties of three steel alloys, International Journal of Automotive and Mechanical Engineering, Vol. 14, No. 2, 2017, pp. 4315-4331, DOI: 10.15282/ijame.14.2.2017.15.0344

[26] Z. Wang, R. Wang, Q. Fei, J. Li, J. Tang, B. Shi, Structure and microscopic wear analysis of lining material based on EDEM, MATEC Web of Conferences, Vol. 128, 2017, Paper 03001, DOI: 10.1051/matecconf/201712803001